Research Square

Preprints are preliminary reports that have not undergone peer review.
They should not be considered conclusive, used to inform clinical practice,
or referenced by the media as validated information.

Rough-Fuzzy Modeling and Interpolation Reasoning with Application in Weld-Penetration Control

Xin Li
Beibu Gulf University
Zhi-Qiang Feng
fzqsjtu@163.com

Beibu Gulf University
Nai-Wen Fang
Harbin Welding Institute Limited Company
Shi-Xian Wu
Guangxi Technological College of Machinery and Electricity

Article

Keywords: Weld-penetration control; Variable-precision tolerance rough set; Knowledge mining; Fuzzy interpolation reasoning; Sparse rule base

Posted Date: November 12th, 2026

DOI: https://doi.org/10.21203/rs.3.rs-11449987/v1

License: This work is licensed under a Creative Commons Attribution 4.0 International License.
Read Full License

Additional Declarations: No competing interests reported.

Rough-Fuzzy Modeling and Interpolation Reasoning with Application in Weld-Penetration Control

Xin Li[a], Zhi-Qiang Feng[a,b,*], Nai-Wen Fang[c] , Shi-Xian Wu[b]

[a]*College of mechanical and marine engineering, Beibu Gulf University, Qinzhou 535011. China;*

[b]*Guangxi Technological College of Machinery and Electricity, Nanning 530000, China;*

[c] *Harbin Welding Institute Limited Company, Harbin 150028, China;*

[*]*Correspondence: fzqsjtu@163.com;*

Abstract

Weld-penetration control is a fundamental problem associated with welding automation. The pursuit of frontal molten-pool features that reflect the penetration information and the establishment of correspondence relationships between the molten state and the representative features of the molten pool are key procedures in achieving real-time penetration control. This article proposes a weld-penetration control method that combines variable-precision tolerance rough set (VPTRS) knowledge mining, fuzzy logic modeling, and interpolation reasoning techniques. A VPTRS model was constructed to address the shortcomings of classical rough sets, which handle continuous and noisy data poorly. A fast-reduction algorithm, which uses feature importance as heuristic information, was proposed. In addition, a rule-extraction algorithm was obtained by partitioning the universe of discourse through tolerance relations. Traditional fuzzy reasoning methods cannot effectively handle reasoning under incomplete rule-base conditions. To address this issue, a fuzzy interpolation reasoning algorithm was developed by extracting the geometric features of fuzzy-set membership functions and calculating feature distance and similarity ratios. Multiple welding experiments were conducted to establish a fusion decision information system. Correspondence relationships between the frontal molten-pool features and the penetration state were obtained from VPTRS feature reduction and rule extraction processes, and a weld-penetration control system was constructed based on fuzzy logic modeling and interpolation reasoning techniques. Welding experiments were also conducted to test the performance of the control system. The results indicated that the formed quality of the weld seam obtained by the proposed method was better than that obtained by ANN-fuzzy control, and that the system performance met the requirements of welding process specifications. The main contribution of this methodology is that it can extract a set of interpretable decision rules from the raw data set collected in the experiment, and then achieve real-time control of the welding penetration process through interpolation reasoning. By using the VPTRS modeling technology, it can be found that certain easily overlooked melt pool characteristics, such as tail width coefficient and tail area coefficient, are closely related to the melting state, which is crucial for achieving melting

control with minimal controlled variables.

Keywords: Weld-penetration control; Variable-precision tolerance rough set; Knowledge mining; Fuzzy interpolation reasoning; Sparse rule base

1. Introduction

Welding is an integral part of manufacturing processes and is widely used in industrial production. Adequate weld penetration is a prerequisite to the achievement of high welding quality, and penetration control is a fundamental issue inherent to welding automation. The melting width on the backside of a weld most directly reflects the penetration condition; however, for many structures, such as pressure vessels and oil pipelines, it is not easy to directly observe the backsides of the weld seams. In addition, when a visual sensor is placed on the back side of the workpiece and is not attached to the welding gun, synchronization between the two is difficult. For these reasons, reliable frontal penetration information has been a topic of exploration for scholars.

In practical operations, experienced welders often obtain penetration information by observing the geometric shape of the frontal molten pool. They then adjust welding electrical parameters based on changes in certain key features of the weld pool to achieve satisfactory penetration formation. It is evident that there is an explicit correspondence between the shape of the frontal melt pool and the state of weld penetration [1]. However, there are dozens of morphological features that can characterize the molten pool, such as the length, width, and area of the weld pool. Therefore, it is crucial to find the potential key features that can characterize the molten state and establish their corresponding relationships for achieving welding penetration control. Rough set theory provides a new feasible approach to solve this problem [2]. Knowledge acquisition is the main application area of rough set theory, which aims to mine implicit knowledge, patterns, and rules from the original dataset of a system, and present them in the form of production rules.

The control algorithm has a significant impact on the effectiveness of penetration control. In terms of intelligent control of welding processes, control algorithms based on fuzzy logic reasoning have been widely recognized for their high adaptability to welding processes. Some classic reasoning methods, such as the Mamdani algorithm and the TKS algorithm, have also been proven to be effective in practical applications [3]. However, the accuracy of the results obtained by these methods is dependent upon the completeness or density of the constructed rule base. When the professional knowledge obtained through human learning or machine learning is incomplete and cannot be used to establish a dense rule base, invalid inference results may be generated. Fuzzy rule interpolation (FRI) provides an effective solution for approximate reasoning under sparse knowledge conditions [4]. Unlike classical compositional rule inference (CRI) and its derivative methods, FRI does not match observations with each rule in the rule base; rather, it implements interpolation inference by selecting the fuzzy rule nearest to the observation. These selected rules form the basis for fuzzy interpolation.

Based on the above problem statement, the motivation of this work is to establish the correspondence between the front features of the melt pool and the melting state through the knowledge acquisition of rough sets, and to

obtain the law of the shape of the melt pool changing with the melting process. Then, interpolation reasoning is used to address the problem of welding penetration control in non-dense rule libraries. The main contribution of the proposed methodology is that it can extract a set of interpretable decision rules from the raw dataset obtained from experiments, and achieve real-time control of the melting process through interpolation reasoning.

The novelty of this work lies in the combination of the concepts of variable precision and tolerance relationship to construct a variable precision tolerance rough set (VPTRS) model, which overcomes the shortcomings of classical rough sets that cannot directly analyze continuous value data and have poor adaptability to noisy data. Next, the knowledge acquisition strategy of VPTRS is used to establish the correspondence between the features of the melt pool and the melting state. In addition, considering that the inference results of classical FRI may not always satisfy the convexity and regularity of the set, an improved interpolation inference method is presented by defining characteristic distance and constructing characteristic similarity ratio.

The remainder of this article is organized into four additional sections. Section 2 briefly reviews relevant literature. Section 3 presents the construction of a VPTRS model and related algorithms for feature reduction and rule extraction. It also discusses an interpolation reasoning method that is based on feature distance and similarity. Section 4 describes the construction of a weld-penetration control system that uses VPTRS, fuzzy logic, and interpolation reasoning algorithms. It also discusses the verification of the relevant models and algorithms, which was accomplished with welding experiments. Section 5 presents the conclusions obtained from the study.

2. Relevant literature

Adequate penetration is one of the most important technical requirements for load-bearing welds. Control of the fusion process, which is a major aspect of welding quality control, has long been a concern in the welding industry. Chen et al. [3] established a fuzzy control model for the molten-pool width. It was based on the proportional relationship between the width of the frontal molten pool and the depth of the overall molten pool. During the welding process, visual inspection was used to detect the width of the molten pool, then the welding parameters were adjusted utilizing fuzzy reasoning to achieve online control of the weld penetration. Xiong and Zou [5] designed a novel active visual-sensing system that consisted of a camera and an auxiliary light source. They also developed corresponding image-processing algorithms to suppress noise and calculate the width of the back weld seam. They prevented incomplete fusion during the welding process by using a fuzzy controller to adjust the welding current. Yan [6] collected images of the front and back of the molten pool using a passive visual-sensing system, analyzed the effects of the primary welding process parameters on the molten pool, and designed a fuzzy PID controller to stabilize the molten pool by adjusting the feed speed of the wire. Li et al. [7] constructed a visual-sensing system to build a 304 stainless-steel FFP-TIG molten pool image dataset, developed a fusion recognition model, and designed a fuzzy controller to adjust the fast-frequency base current in real-time, thereby achieving closed-loop control of the fusion state. Pan [8] used visual inspection to monitor the front and back weld surfaces during a welding process in real-time, obtained the corresponding relationship between the size

of the molten pool and the penetration of the weld seam, and established a fuzzy control system in which the feed speed of the wire was the control variable and the size of the frontal molten pool was the controlled variable. Thus, penetration control during the welding process was achieved by the use of fuzzy control.

Liu et al. [9] developed an adaptive neural fuzzy inference system to simulate the intelligence of human welders. This was done to process visual information from the molten pool and adjust the welding parameters. Wang et al. [10] designed a penetration control strategy for step welding that was based on characteristic signals that reflected the degree of penetration. They used these characteristic signals along with back-propagation (BP) neural networks to dynamically model the width of the back molten pool. By using this step-welding control strategy and real-time feedback predicted by the BP neural networks, the width of a horizontally oriented back weld seam could be controlled near a preset value. Bai [11] used the structural laser reflection method and electrical-signal in-formation from multiple sensors to capture peak-period laser-reflection fringes under different fusion states. They also analyzed the continuous-welding fusion law. Research has revealed that both the arc-voltage fluctuations and the average value of the arc voltage during the peak-pulse stage can reflect whether weld penetration has occurred. Different characteristic quantities can be used for weld-penetration control in different welding processes. Chen et al. [12] used computer vision methods to extract key features related to three-dimensional molten-pool surface features and established a database that spanned a wide range of welding conditions. A feature importance analysis revealed that the width of the molten pool, the length of the trailing edge, and the surface height all affected predictions of the back molten-pool width. Their results laid foundation for the further establishment of real-time closed-loop weld-penetration control systems.

The rough-set theory, which is an effective tool for knowledge mining, can discover hidden patterns and rules from large amounts of data. This capability has led to its application to welding process modeling and process modeling. Li et al. [13] used a rough-set method to fuse arc-sensor information with visually obtained information to predict the groove state. Chen [14] employed rough-set modeling to model a small group of welding process parameters and obtained relationships between these welding process parameters and the welding accuracy deviation by using the variable-precision rough-set theory. Li et al. [15] developed a modeling method that was based on rough sets to extract the weld deviation, obtained sufficient experimental data under different deviation conditions, and established a decision information table. This decision table was discretized and the number of its attributes was reduced by using rough sets to obtain a fuzzy knowledge model for weld-deviation control. Zhong [16] established a rough-set multi-information fusion model using a variety of information types, such as the current, voltage, wire feed speed, frontal molten-pool image information, and sound information. The model accurately predicted the back width of a weld seam generated by pulsed GTAW of an aluminum alloy. Chao and Sun [17] analyzed attributes related to welding types, established a decision table for welding-type selection, used rough-set attribute reduction to remove attributes that did not affect the welding-type selection, and improved the accuracy and reliability of subsequent rule extraction. Wang et al. [18] introduced the theory of neighborhood

rough sets to analyze the factors that affected the fatigue lives of aluminum-alloy welded joints. An algorithm that combined forward-greedy and back-ward pruning was used for attribute reduction to obtain the core set of factors that affected the joint fatigue life. Jiang [19] combined an improved fish swarm-based neighborhood rough-set attribute-reduction algorithm to establish an evaluation model for the factors that affected the fatigue lives of aluminum-alloy welded joints and developed a system to evaluate these factors.

The welding process is a typical complex process and is characterized by time variance, nonlinearity, and a multiplicity of interfering factors; thus, it is difficult to establish an accurate mathematical model for this process. Fuzzy logic control can mimic human operations, is very robust, and has good flexibility. It has been successfully applied to the control of intermediate welding processes, such as weld formation and weld tracking [20-22]. Fuzzy reasoning is an important component in the development of fuzzy control systems. Existing reasoning algorithms, such as the Mamdani algorithm, the TSK algorithm, and the similarity-based reasoning algorithm, can only produce reasonable and accurate results when the rule base is dense or complete. However, in practical applications, due to incomplete domain knowledge or a reduction in the number of rules to decrease the system complexity, the rule base may be sparse or incomplete. Kóczy and Hiro-ta [23] were the first scholars to propose an FRI reasoning method to address the need for classical reasoning methods for a dense rule library during the application process. After that, various fuzzy interpolation reasoning algorithms emerged successively, thereby indicating that this method had become an important inference method, following Zadeh's CRI method and Turksen's similarity-based approximation reasoning (SAR) method.

Some achievements have also been made with respect to the FRI application. Guo et al. [24] employed a fuzzy interpolation reasoning method to diagnose local defects in electrical equipment. They also applied an interpolation reasoning method to the feature areas of ultra-high-frequency signals in partial discharge to improve the system sampling rate. Molnárka et al. [25] proposed an FRI method to describe the states of residential buildings in response to the large number of rules generated by multi-component building types; this method reduced the number of these rules to a reasonable and manageable quantity. Ofor et al. [26] used FRI technology to achieve face detection and expression recognition. Szili et al. [27] adopted fuzzy interpolation reasoning to achieve speed control of mobile robots with only a small number of rules. Yang et al. [28] proposed an ANFIS construction method that was based on sparse data to achieve interpolation between AN-FIS. This method decomposed the ANFIS so that it could be interpolated into a set of fuzzy rules, and then performed rule interpolation in the form of rule clusters. The intermediate rules obtained from the interpolation were used to construct a new ANFIS. Li et al. [29] used an attribute-weighted FRI method to construct a CADx system for the mass classification of breast X-ray images. When unknown mass observations did not match any rules in the rule library, the system could derive a conclusion based on interpolation reasoning.

According to the literature survey mentioned above, the main approach for welding penetration control is to use machine-learning algorithms such as artificial neural networks (ANNs) to establish relationships between

various welding parameters (inputs) and the back molten-pool width (output). Thus, they can be used to predict and control the back molten-pool width by conducting real-time detection of multiple parameters during the welding process [30]. However, when using these models, it is difficult to determine which parameters are inherently related to the fusion state and should therefore be added to the inputs. In addition, selection of the key parameters of ANN models, such as the number of hidden-layer nodes, the learning rate, and the number of iterations, is largely dependent on experience and experimentation; thus, it limits the model application potential.

The objective of this article is to use the knowledge acquisition strategy of variable-precision tolerance rough sets to establish the correspondence between the key features of the frontal weld pool and the penetration state. Variable- precision tolerance rough set is an extended model of classical rough set, which enhances the adaptability of the model to continuous value data with noise by combining variable precision and tolerance relation. In addition, an improved fuzzy interpolation reasoning algorithm is adopted to address the problem of sparse melting control rules and inability to match rules. The algorithm can reduce the complexity of the algorithm by simplifying the representation of membership functions, constructing characteristic distances and similarity ratios, and its conclusions can satisfy the basic properties of multi-dimensional reasoning.

3. Methodology

3.1. Two extended rough-set models

The classical Pawlak rough-set model can only handle discrete and crisp data, and it lacks the ability to resist noise and interference; these deficiencies add certain difficulty to its application. Researchers have extended classical rough sets from different perspectives, thereby forming a variety of extended rough-set models [2].

In the model, $(U, C \bigcup \{d\})$ represents a decision information system, where U is a set of finite objects, called the universe of discourse, or universe. C is a set composed of multiple conditional features and is referred to as a conditional feature set, while d is a decision feature.

The equivalence relation between the objects in a Pawlak rough set is reflexive, symmetric, and transitive. In practical applications, however, the continuity of data makes it impossible for the relations between objects to meet these strict equivalence standards.. To enable rough sets to directly process continuous data, Skowron et al. weakened the equivalence relation in a Pawlak rough set such that it became a tolerance relation and proposed a tolerance rough-set model (TRS) [31].

T is defined as a binary relation on U. If $(x, x) \in T$ for any $x \in U$ (reflexivity) and $(x, y) \in T \leftrightarrow (y, x) \in T$ for any $x, y \in U$ (symmetry), then T is called a tolerance relation on U.

By defining the similarity between objects in U and setting the corresponding threshold, τ, a tolerance relation could be constructed in the decision information system. $a \in C$ represents a conditional feature in $(U, C \bigcup \{d\})$. For any $x, y \in U$, the similarity degree between x and y with respect to a can be expressed by Eq. (1):

$$S_a(x, y) = 1 - \frac{|a(x) - a(y)|}{a_{\max} - a_{\min}} \quad (1)$$

where $a_{\max} = \max_{z \in U} a(z)$ and $a_{\min} = \min_{z \in u} a(z)$ represent the maximum and minimum feature values of the object in U with respect to a, respectively.

$T_{a,\tau}$ is defined as a binary relation on U that is derived from a, and $\tau \in (0,1]$. If Eq. (2) is satisfied, then $T_{a,\tau}$ is called the τ-tolerance relation on U with respect to a:

$$T_{a,\tau} = \left\{ (x,y) \in U \times U \middle| S_a(x,y) \geq \tau \right\} \tag{2}$$

Obviously, $T_{a,\tau}$ satisfies both reflexivity and symmetry.

$B \subseteq C$ is a conditional feature subset in $(U, C \bigcup \{d\})$ and $\tau \in (0,1]$. For any $a \in B$, if Eq. (3) is satisfied, then $T_{B,\tau}$ is also a tolerance relation that is referred to as the τ-tolerance relation on U with respect to B:

$$T_{B,\tau} = \bigcap_{a \in B} T_{a,\tau} = \left\{ (x,y) \in U \times U \middle| \min_{a \in B} S_a(x,y) \geq \tau \right\} \tag{3}$$

By using $T_{a,\tau}$ from Eq. (3) to perform fuzzy partitioning, $U/T_{B,\tau}$, on U, a set of tolerance classes can be generated that satisfy Eq. (4):

$$\begin{cases} U/T_{B,\tau} = \left\{ S_{B,\tau}(x) \middle| x \in U \right\} \\ S_{B,\tau}(x) = \left\{ y \in U \middle| (x,y) \in T_{B,\tau} \right\} \end{cases} \tag{4}$$

In Eq. (4), $S_{B,\tau}(x)$ is the τ-tolerance class of x with respect to B, which is a conditional tolerance class derived from B. Obviously, the set of tolerance classes obtained from $U/T_{B,\tau}$ usually constitutes coverage of U.

The classification produced by Pawlak rough sets is an accurate classification that is based on a complete inclusion relation between sets; this relation does not allow any misclassification, which causes the rough sets to lack adaptability to noisy data in practical applications. To overcome this drawback, Ziarko et al. proposed a variable-precision rough-set model by introducing the concept of a misclassification rate [32]. In this model, the complete inclusion relation between sets was changed so that it became a majority inclusion relation. Upper and lower approximations with different precision could be obtained by changing the threshold, *β*, of the misclassification rate, which provided the model with a certain degree of noise resistance and fault tolerance.

U is defined as a finite universe that is not empty. $\rho : U \times U \to [0,1]$ is a binary function that satisfies Eq. (5):

$$\rho(X,Y) = \begin{cases} 1 - \dfrac{Card(X \bigcap Y)}{Card(X)}, & X \neq \varnothing \\ 0, & X = \varnothing \end{cases} \tag{5}$$

If Eq. (5) holds for any $X, Y \subseteq U$, then $\rho(X,Y)$ is called the misclassification rate of X with respect to Y. In Eq. (5), $Card(\cdot)$ represents the cardinality of a set, while $Card(X \bigcap Y)/Card(X)$ is the inclusion degree of X in Y (i.e., the correct classification rate of X with respect to Y).

2.2 Variable-precision tolerance rough set and knowledge mining

In welding information systems, most data has continuity and contains a certain degree of noise. To enhance the adaptability of rough sets to welding processes, an extended rough-set model that combines variable precision

and tolerance relations, referred to as a variable-precision tolerance rough-set (VPTRS), is presented during this study.

Recall the decision information system $(U, C \bigcup \{d\})$ and $B \subseteq C$. $T_{B,\tau}$ is the τ-tolerance relation on U with respect to B and $S_{B,\tau}(x)$ is the τ-tolerance class of x with respect to B. $\beta \in [0, 0.5)$ is the threshold of the misclassification rate. For any $X \subseteq U$, the variable-precision tolerance β-lower and β-upper approximations of X with respect to B are given by Eq. (6):

$$\begin{cases} \underline{T}_{B,\tau}^{\beta}(X) = \left\{ x \in U \middle| \rho(S_{B,\tau}(x), X) \le \beta \right\} \\ \overline{T}_{B,\tau}^{\beta}(X) = \left\{ x \in U \middle| \rho(S_{B,\tau}(x), X) < 1 - \beta \right\} \end{cases} \tag{6}$$

Eq. (6) indicates that, after the introduction of the variable-precision concept in the tolerance rough-set model, the variable-precision tolerance β-lower approximation of X with respect to B is a set of tolerant conditional classes for which the misclassification rate of X is not greater than β and the variable-precision tolerance β-upper approximation of X with respect to B is a set of tolerant conditional classes where the misclassification rate of X^c (the complement of X) is not less than β.

The variable-precision tolerance β-positive, β-boundary, and β-negative regions of X with respect to B are given by Eq. (7):

$$\begin{cases} Pos_{B,\tau}^{\beta}(X) = \underline{T}_{B,\tau}^{\beta}(X) \\ = \left\{ x \in U \middle| \rho(S_{B,\tau}(x), X) \le \beta \right\} \\ Bnd_{B,\tau}^{\beta}(X) = \overline{T}_{B,\tau}^{\beta}(X) \setminus \underline{T}_{B,\tau}^{\beta}(X) \\ = \left\{ x \in U \middle| \beta < \rho(S_{B,\tau}(x), X) < 1 - \beta \right\} \\ Neg_{B,\tau}^{\beta}(X) = \left\{ x \in U \middle| \rho(S_{B,\tau}(x), X) \ge 1 - \beta \right\} \end{cases} \tag{7}$$

if $Bnd_{B,\tau}^{\beta}(X) \neq \varnothing$, then $\underline{T}_{B,\tau}^{\beta}(X) \neq \overline{T}_{B,\tau}^{\beta}(X)$; Otherwise, $\underline{T}_{B,\tau}^{\beta}(X) = \overline{T}_{B,\tau}^{\beta}(X)$ and $Pos_{B,\tau}^{\beta}(X) \bigcup Neg_{B,\tau}^{\beta}(X) = U$.

$U/d = \{Y_1, Y_2, \cdots, Y_r\}$ is the set of decision equivalence classes derived from the decision feature d. The variable-precision tolerance β-relative positive region of d with respect to B can be expressed by Eq. (8):

$$\begin{aligned} Pos_{B,\tau}^{\beta}(d) &= \bigcup_{Y_j \in U/d} \underline{T}_{B,\tau}^{\beta}(Y_j) \\ &= \bigcup_{Y_j \in U/d} \left\{ x \in U \middle| \rho(S_{B,\tau}(x), Y_j) \le \beta \right\} \end{aligned} \tag{8}$$

The variable-precision tolerance β-approximate classification quality of d with respect to B is expressed by Eq. (9):

$$\gamma_{B,\tau}^{\beta}(d) = Card(Pos_{B,\tau}^{\beta}(d)) / Card(U) \tag{9}$$

The approximate classification quality (also known as the approximate dependency) reflects the proportion of objects in U that accurately partitions each conditional tolerance class into each decision equivalence class under the condition that the misclassification rate is not greater than β.

Feature reduction (also known as feature selection) is the core concept and one of the most widely used applications of the rough-set theory. It can eliminate unnecessary or irrelevant redundant conditional features while maintaining the classification capability of the conditional features in decision information systems.

Given $(U, C \bigcup \{d\})$ and $\beta \in [0, 0.5)$. For any $B \subseteq C$ and $B' \subset B$, if Eq. (10) is satisfied, then B is referred to as a variable-precision tolerance β-reduction of C relative to d and is denoted as $Red_{d,\tau}^{\beta}(C)$:

$$\begin{cases} 1)\ \gamma_{B,\tau}^{\beta}(d) = \gamma_{C,\tau}^{\beta}(d) \\ 2)\ \gamma_{B',\tau}^{\beta}(d) \neq \gamma_{C,\tau}^{\beta}(d) \end{cases} \tag{10}$$

Eq. (10) indicates that the purpose of feature reduction is to find a minimum subset of conditional features from C that has the same approximate classification quality as the original decision information system.

Feature importance is a key concept in rough-set knowledge reduction. It determines which conditional features should be selected and retained in a minimum feature subset during the reduction process. Given $(U, C \bigcup \{d\})$ and $\beta \in [0, 0.5)$. For any $a \in C$, the importance of a relative to d in C is expressed by Eq. (11):

$$Sig(a, C, d, \beta, \tau) = \gamma_{C,\tau}^{\beta}(d) - \gamma_{C \setminus \{a\},\tau}^{\beta}(d) \tag{11}$$

Eq. (11) represents the proportion of objects in U that cannot be classified correctly after removing feature a from C provided that the misclassification rate is not greater than β.

Next, the feature importance and the increment in the approximate classification quality can be taken as heuristic information, and the addition method can be used to calculate the feature reduction of the decision information system.

Algorithm 1: Feature reduction based on a variable precision tolerance rough set

Input: $(U, C \bigcup \{d\})$, β, and τ

Output: β–reduction, Red

Step1: The importance, $Sig(a, C, d, \beta, \tau)$, and approximate classification quality, $\gamma_{C,\tau}^{\beta}(d)$, of each feature, $a \in C$, are calculated.

Step2: $Red \leftarrow \varnothing$ is performed. The feature with the maximum importance is selected according to $b = \text{argmax}_{a \in C} Sig(a, C, d, \beta, \tau)$ and $Red \leftarrow Red \bigcup \{b\}$.

Step3: The approximate classification quality, $\gamma_{Red,\tau}^{\beta}(d)$, is calculated.

Step4: If $\gamma_{Red,\tau}^{\beta}(d) = \gamma_{C,\tau}^{\beta}(d)$,then the model proceeds to Step7. Otherwise, the model continues to Step5.

Step5: The approximate classification quality, $\gamma_{Red \bigcup \{a\},\tau}^{\beta}(d)$, is calculated for each $a \in C \setminus Red$.

Step6: The feature with the maximum approximate classification quality is selected according to $c = \text{argmax}_{a \in C \setminus Red} \gamma_{Red \bigcup \{a\},\tau}^{\beta}(d)$ and $Red \leftarrow Red \bigcup \{c\}$ .Then the model proceeds to Step3.

Step7: β-reduction, Red, is output and the algorithm ends.

In addition to feature reduction, another major application of the rough-set theory is to obtain explicit knowledge in the form of if–then statements from decision information systems through inductive learning; Therefore, simplified knowledge models can be established.

$(U, Red \bigcup \{d\})$ is defined as a reduced decision information system and $U/Red = \{S_i \mid i = 1, 2, \cdots, m\}$ is the set of conditional tolerance classes derived from the minimum reduction, Red, while $U/d = \{Y_j \mid j = 1, 2, \cdots, n\}$ is the set of decision equivalence classes derived from d. For any $x \in U$, if $x \in S_i$ and $x \in Y_j$, then the descriptions of S_i and Y_j in $(U, Red \bigcup \{d\})$ are given by Eq(12):

$$\begin{cases} Des(S_i) = \underset{a \in Red}{\wedge}(a,\ a(x)) \\ Des(Y_j) = (d,\ d(x)) \end{cases} \tag{12}$$

where $a(x)$ and $d(x)$ are the feature values of x with respect to a and d, respectively.

$Conf_{ij} = Card(S_i \bigcap Y_j)/Card(S_i)$ is also defined as the confidence level of the rule. For a threshold of $\xi \in (0,1]$, the classification rule, r_x, for x that is obtained by $(U, Red \bigcup \{d\})$ can be expressed by Eq. (13):

$$r_x :\ Des(S_i) \to Des(Y_j) \quad (Conf_{ij}) \tag{13}$$

where $Conf_{ij} \geq \xi$, while $Des(S_i)$ and $Des(Y_j)$ represent the antecedent and consequent of the rule, respectively.

Eqs. (12) and (13) demonstrate that a set of threshold-constrained classification rules can be generated in the reduced decision information system by using the tolerance relation between objects to derive conditional tolerance classes and then calculating the rule confidence.

Algorithm 2: Rule acquisition based on the tolerance relation

Input: $(U, Red \bigcup \{d\})$, τ, and ξ

Output: $RuleSet$

Step1: $RuleSet \leftarrow \varnothing$ is performed, then

$U/Red = \{S_1, S_2, \cdots, S_m\}$ and $U/d = \{Y_1, Y_2, \cdots, Y_n\}$ are calculated.

Step2: The confidence, $Conf_{ij}$ $(i = 1, 2, \cdots, m;\ j = 1, 2, \cdots, n)$, is calculated.

Step3: If $Conf_{ij} \geq \xi$, then

$RuleSet \leftarrow RuleSet \bigcup \{Des(S_i) \to Des(Y_j)\ \ (Conf_{ij})\}$.

Step4: $RuleSet$ is output and the algorithm ends.

3.3 Interpolation reasoning based on characteristic distance and similarity

Traditional fuzzy reasoning methods, such as the CRI, Mamdani, and TSK algorithms, require the rule base to be complete or dense. However, if complete professional knowledge is difficult to obtain, the fuzzy rule base may become sparse or incomplete. When the input value fails to trigger any rules in the base, inappropriate or invalid inference results are obtained. The emergence of FRI technology has removed the key limiting conditions that are present in classical reasoning methods. Since Kóczy and Hirota proposed the famous linear interpolation inference method, researchers have successively proposed the HCL algorithm, the similarity interpolation algorithm, the

Lagrange algorithm, the centroid interpolation algorithm, and the Newton algorithm. However, these methods have certain limitations, including complexity, large computational loads, the inability to preserve the convexity and normality of the conclusions, inaccurate results under multi-dimensional conditions, and application difficulty [4].

Beginning with the geometric characteristics of the membership function of a polygonal fuzzy set, a set of characteristic points that describe the important geometric features of the fuzzy set could be obtained by finite segmentation of its branches, thereby simplifying the representation of the membership function. On this basis, a fuzzy interpolation inference algorithm was developed by defining a fuzzy-set feature distance and a feature similarity ratio.

A is defined as a fuzzy set with polygonal membership function (also known as a polygon fuzzy set) on the universe X, while $k \geq 2$, $l \geq 1$. In addition, $a_1 = \inf\{A_{\alpha=0}\}$, $a_k = \inf\{A_{\alpha=1}\}$, $a_{k+1} = \sup\{A_{\alpha=1}\}$, and $a_{k+l+1} = \sup\{A_{\alpha=0}\}$ are defined, where $A_{\alpha=0}$ and $A_{\alpha=1}$ are the 0-cut set and the 1-cut set of A, respectively. $k-1$ divisions are made at the turning point of the polygon between a_1 and a_k; this set of division points is denoted as $\{a_1, a_2, \cdots, a_k\}$. Next, l divisions are made at the turning point of the polygon between a_{k+1} and a_{k+l+1}, and this set of division points is denoted as $\{a_{k+1}, a_{k+2}, \cdots, a_{k+l+1}\}$. Then $\{a_1, a_2, \cdots, a_k, a_{k+1}, a_{k+2}, \cdots, a_{k+l+1}\}$ is defined as the characteristic point set of A or the characteristic of A; it is denoted as $Char(A)$.

For example, for a normal triangular fuzzy set, the characteristic of A can be expressed as $Char(A) = \{a_1, a_2, a_3\}$, where a_1 and a_3 are the left and right endpoints of the branch set of A and a_2 is the kernel of A. For a normal trapezoidal fuzzy set, $Char(A) = \{a_1, a_2, a_3, a_4\}$, where a_2 and a_3 are the kernels of A.

If A and B are polygonal fuzzy sets on the universe X, then their characteristics can be expressed by $Char(A) = (a_1, a_2, \cdots a_m)$ and $Char(B) = (b_1, b_2, \cdots b_m)$. If D is a binary function that satisfies Eq. (14), then $D(A, B)$ is referred to as the characteristic distance between A and B:

$$D(A,B) = \left[\sum_{k=1}^{m} (a_k - b_k)^2\right]^{1/2} \quad (14)$$

Given the polygonal fuzzy sets A and B on X, if Eq. (15) holds for $k = 1, 2\cdots, m-1$, where $wid^k(A)$ and $wid^k(B)$ are the kth characteristic widths of A and B and satisfy Eq. (16), then $S_k(A, B)$ is referred to as the kth characteristic similarity ratio of A and B:

$$S_k(A,B) = \frac{wid^k(A)}{wid^k(B)} \quad (15)$$

$$wid^k(A) = a_{k+1} - a_k,\ wid^k(B) = b_{k+1} - b_k \quad (16)$$

Specifically, for triangular fuzzy sets A and B, Eq. (17) could be obtained:

$$S_L(A,B) = \frac{a_2 - a_1}{b_2 - b_1},\ S_R(A,B) = \frac{a_3 - a_2}{b_3 - b_2} \quad (17)$$

where $S_L(A, B)$ and $S_R(A, B)$ are the left and right characteristic similarity ratios, respectively.

If A_1 and A_2 are polygonal fuzzy sets on X, then for any $\alpha \in [0,1]$, if $\inf\{A_{1\alpha}\} < \inf\{A_{2\alpha}\}$ and $\sup\{A_{1\alpha}\} < \sup\{A_{2\alpha}\}$, then $A_1 < A_2$, where $A_{1\alpha}$ and $A_{2\alpha}$ are the α-cut sets of A_1 and A_2, respectively.

Next, taking common multi-dimensional reasoning as an example, an interpolation reasoning method that is based on characteristic distance and similarity (CDS) is presented. In this example, all the fuzzy sets are triangular. Here, A_{1i}, A_{2i}, and A_i^* are defined as the fuzzy sets on the universe X_i $(i = 1, 2\cdots, n)$ and B_1, B_2, and B^* are defined as the fuzzy sets on the universe Y, where $A_{1i} < A_i^* < A_{2i}$ $(i = 1, 2\cdots, n)$. The following inference model is used for the subsequent discussion:

Rule 1:	$A_{11} \wedge A_{12} \wedge \cdots \wedge A_{1n} \rightarrow B_1$
Rule 2:	$A_{21} \wedge A_{22} \wedge \cdots \wedge A_{2n} \rightarrow B_2$
Observation:	$A_1^* \wedge A_2^* \wedge \cdots \wedge A_n^*$
Conclusion:	B^*

Feature points are extracted according to the shape of the fuzzy sets for $i = 1, 2\cdots, n$:

$$Char(A_{1i}) = (a_{11}^i, a_{12}^i, a_{13}^i),\ Char(A_{2i}) = (a_{21}^i, a_{22}^i, a_{23}^i),$$

$$Char(A_i^*) = (a_{i1}^*, a_{i2}^*, a_{i3}^*),\ Char(B_1) = (b_{11}, b_{12}, b_{13}),$$

$$Char(B_2) = (b_{21}, b_{22}, b_{23}), \text{ and } Char(B^*) = (b_1^*, b_2^*, b_3^*).$$

The characteristic distance ratio is calculated. Eq. (14) indicates that, for $i = 1, 2, \cdots, n$, the characteristic distances between A_{1i} and A_i^*, and between A_{1i} and A_{2i},can be expressed by Eqs. (18) and (19):

$$D(A_{1i}, A_i^*) = \left[\sum_{j=1}^{3} (a_{1j}^i - a_{ij}^*)^2\right]^{1/2} \quad (18)$$

$$D(A_{1i}, A_{2i}) = \left[\sum_{j=1}^{3} (a_{1j}^i - a_{2j}^i)^2\right]^{1/2} \quad (19)$$

Then, the characteristic distance ratio, λ_D^i,can be obtained from Eq. (20):

$$\lambda_D^i = D(A_{1i}, A_i^*) / D(A_{1i}, A_{2i}) \quad (20)$$

The antecedent, $A_i'(i = 1, 2, \cdots, n)$, and the consequent, B', of a new rule are constructed according to the characteristic distance ratio. If $Char(A_i') = (a_{i1}', a_{i2}', a_{i3}')$ and $Char(B') = (b_1', b_2', b_3')$, then, for $i = 1, 2, \cdots, n$ and $j = 1, 2, 3$, Eq. (21) can be obtained from Eq. (20):

$$a_{ij}' = (1 - \lambda_D^i) a_{1j}^i + \lambda_D^i a_{2j}^i \quad (21)$$

If $\lambda_D = \sum_{i=1}^{n} \lambda_D^i / n$ is the comprehensive characteristic distance ratio, then, for $j = 1, 2, 3$, Eq. (22) can be obtained:

$$b_j' = (1 - \lambda_D) b_{1j} + \lambda_D b_{2j} \quad (22)$$

A new inference model is established using the constructed rules. According to the rules, $A_1' \wedge A_2' \wedge \cdots \wedge A_n' \rightarrow B'$, which are obtained from steps 1–3, the original inference model can be transformed into the following new inference model:

New rule:	$A_1' \wedge A_2' \wedge \cdots \wedge A_n' \rightarrow B'$
Observation:	$A_1^* \wedge A_2^* \wedge \cdots \wedge A_n^*$

Conclusion:	B^*

The characteristic similarity ratio is computed. Using Eqs. (15)–(17), the left and right similarity ratios of each antecedent of the new rule to the corresponding observed value can be obtained for $i = 1, 2, \cdots, n$ by Eqs. (23) and (24), respectively:

$$S_L(A_i', A_i^*) = (a_{i2}' - a_{i1}') / (a_{i2}^* - a_{i1}^*) \tag{23}$$

$$S_R(A_i', A_i^*) = (a_{i3}' - a_{i2}') / (a_{i3}^* - a_{i2}^*) \tag{24}$$

If $A' = [A_1', A_2', \cdots, A_n']$ and $A^* = [A_1^*, A_2^*, \cdots, A_n^*]$, then the left and right comprehensive similarity ratios of A' and A^* can be obtained from Eqs. (25) and (26), respectively:

$$S_L(A', A^*) = \frac{1}{n} \sum_{i=1}^{n} S_L(A_i', A_i^*) \tag{25}$$

$$S_R(A', A^*) = \frac{1}{n} \sum_{i=1}^{n} S_R(A_i', A_i^*) \tag{26}$$

The membership function characteristics of the conclusion B^* are computed. If $D(B_1, B^*) = D(B_1, B')$ and the left and right similarity ratios of B' and B^* are equal to the left and right comprehensive similarity ratios of A' and A^*, respectively, then Eq. (27) is applicable:

$$\begin{cases} D(B_1, B^*) = D(B_1, B') \\ S_L(B', B^*) = S_L(A', A^*) \\ S_R(B', B^*) = S_R(A', A^*) \end{cases} \tag{27}$$

According to Eq. (14), there will be two solutions for the system of equations in Eq. (27). From the expression $A_{1i} < A_i^* < A_{2i} (i = 1, 2 \cdots, n)$, the relation $B_1 < B^* < B_2$ can be inferred; thus, the unique solution (b_1^*, b_2^*, b_3^*) is obtained.

It can be verified that the proposed CDS reasoning method possesses the following properties: for $i = 1, 2 \cdots, n$,,

1) $D(A_{1i}, A_i^*) = D(A_{1i}, A_i')$.

2) If all the known fuzzy sets are normal convex fuzzy sets, then the obtained conclusion is also a normal convex fuzzy set (normal convexity).

3) If $A_i^1 < A_i^2$, then $f(\wedge_{i=1}^n A_i^1) < f(\wedge_{i=1}^n A_i^2)$ (monotonicity).

4) If $A_i^* = A_{1i}$, then $f(\wedge_{i=1}^n A_i^*) = B_1$ (reducibility).

Next, an example of two-dimensional reasoning is used to illustrate the CDS-based algorithm. This example uses the following inference model:

Rule 1:	$A_{11} \wedge A_{12} \to B_1$
Rule 2:	$A_{21} \wedge A_{22} \to B_2$
Observation:	$A_1^* \wedge A_2^*$
Conclusion:	B^*

In this model, A_{1i} , A_{2i} , and A_i^* are fuzzy sets on the universe X_i and $A_{1i} < A_i^* < A_{2i}$ for $i = 1, 2$. B_1 and B_2 are fuzzy sets on the universe Y . The membership functions of each fuzzy set are triangular membership functions, as shown in Figure 1(a) and 1(b). The characteristics of each fuzzy subset are shown in Table 1.

Table 1 Characteristics of each fuzzy subset

Sets	Char	Sets	Char	Sets	Char	Sets	Char
A_{11}	(1,3,7)	A_{12}	(5,9,13)	A_{21}	(20,25, 27)	A_{22}	(27,30,36)
A_1^*	(10,14,16)	A_2^*	(18, 20,25)	B_1	(10,15,23)	B_2	(45,48,55)

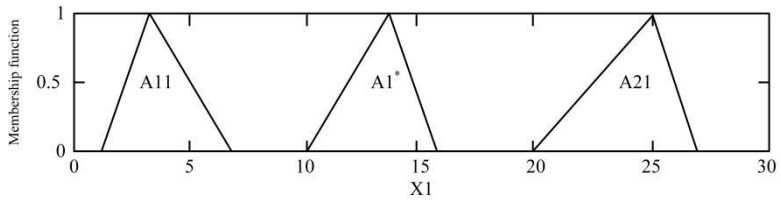
The CDS algorithm was used to obtain the characteristics of the antecedent and consequent of the new rule:

$$Char(A_1') = (10.03, 13.46, 16.51) ,$$

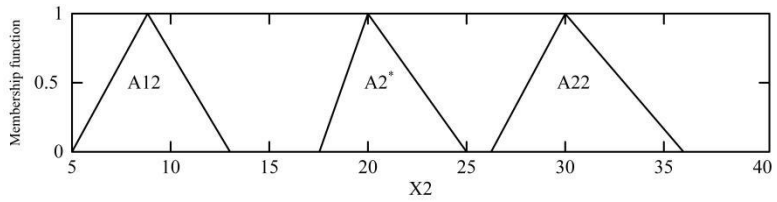
$$Char(A_2') = (17, 20.45, 25.55) ,$$

and $Char(B') = (27.87, 31.84, 39.33)$.

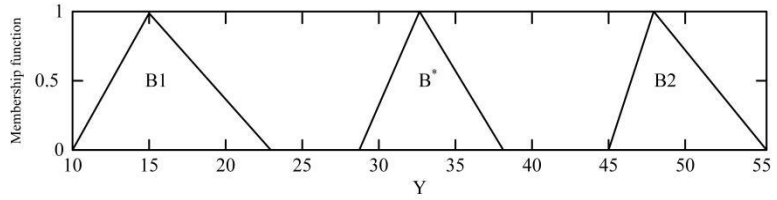
Further calculation yielded Char(B*)=(28.65, 32.13, 38.26). In addition, Figure 1(c) indicates that the method has good applicability with respect to multi-dimensional inference.



(a)



(b)



(c)

Fig.1. Membership functions of the fuzzy sets in the two -dimensional inference model: (a) fuzzy subsets on the universe X_1 , (b) fuzzy subsets on the universe X_2 , and (c) fuzzy subsets on the universe Y .

4. Rough fuzzy model and interpolation reasoning for weld-penetration control

Penetration control is a fundamental welding-automation issue. In the actual welding process, a skilled operator can determine the current penetration situation by observing the shape of the frontal molten pool. The

operator can then adjust the welding parameters to control the penetration depth. Welders have this determination capability because they have found the relationships between certain characteristics of the frontal molten pool and the penetration state through repeated practice or learning. Therefore, simulating the learning process undergone by welders and seeking frontal molten-pool feature information that can reflect the penetration state is crucial to the achievement of intelligent penetration control.

This section describes the knowledge-mining method, which was based on a VPTRS, that was used to establish the relationships between the frontal features of the molten pool and the penetration state. It also describes how, by taking the parameters of the frontal molten pool as the controlled objects, a control model was established using fuzzy logic techniques. To address the issue of sparse control rules, the proposed CDS interpolation algorithm was employed in the inference process. Finally, the experiments that were conducted to test the effectiveness of the relevant models and algorithms are discussed.

4.1 Acquisition of the modeling data

To obtain frontal molten pool features that could characterize the fusion state, welding experiments that were related to the fusion state were conducted during this study. Many welding process factors affect the fusion state. These include both welding conditions, such as the root gap, the groove angle, the thickness of the root face, and the alignment tolerance, and welding specifications, such as the welding current, the welding speed, and the arc voltage. Of these, the most important factors are the root gap and the welding current. Therefore, in the experiments, a variety of fusion states were obtained by changing the root gap and the current, and visual-sensing equipment was used to obtain the feature information of the frontal molten pool. In this way, connections could be established between the features of the frontal molten pool and the fusion state. The primary process parameters used in the experiments are provided in Table 2.

Table 2. Primary process parameters of the welding experiments

Parameter name	Value	Parameter name	Value
Welding method	MAG	Wire material	H08MnSiA
Material	Q235 mild steel	Wire diameter/mm	1.2
Workpiece size /mm3	300×150×6	Welding speed /cm/min	47
Joint type	Butt joint	Arc voltage/V	21
Groove angle/°	60	Welding shielding gas	80% CO2+ 20% Ar
Root face thickness/mm	1.5	Shielding gas flow /L/min	15
Root gap/mm	0.4,0.7,1.2,1.7, 2.0	Welding current/A	155,165,185,205,215

A dynamic welding process monitoring platform, which was based on visual sensing, was built to obtain real-time feature information from the frontal molten pool, as shown in Figure 2. During the welding process, images of the frontal molten pool that were captured by the CCD camera were subjected to image processing tasks, such as filtering and denoising, threshold segmentation, and edge smoothing, to obtain the contour of the molten pool, as shown in Figure 3. The sampling frequency of the CCD camera was 25 Hz. Using parameterized calculations of the molten pool contour, seven geometric feature parameters of the frontal molten pool were extracted. These parameters are the tail length, c1, the maximum width, c2, the tail length-to-width ratio, c3, the tail area, c4, the tail-area ratio, c5, the trailing angle, c6, and the tail-width ratio, c7.

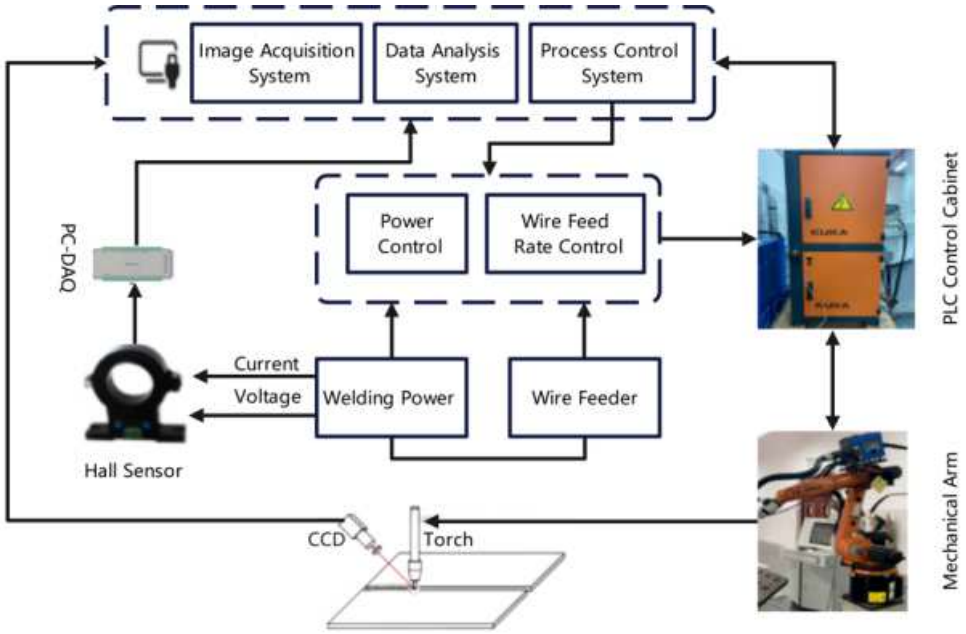


Fig.2.Dynamic welding process monitoring platform based on visual sensing

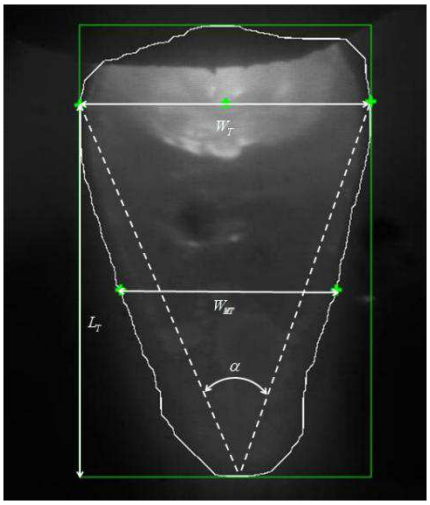


Fig.3. Frontal molten-pool contour and related feature parameters

According to rough-set knowledge representation, an information system could be established using the weld penetration state as the decision feature, as shown in Table 3. This system was a two-dimensional information model composed of sample objects u_1–u_{23}, conditional features c_1–c_7, and decision feature d. In this table, decision feature values of −1, 0, and 1 represent the incomplete penetration, complete penetration, and excessive penetration states, respectively.

Table 3 Decision information system for the weld penetration type

U	c_1	c_2	c_3	c_4	c_5	c_6	c_7	d
u_1	203	227	1.0557	34264	0.740344	58.3858	0.817982	−1
u_2	227	246	1.11908	40220	0.718398	56.9552	0.794792	−1
u_3	287	279	1.24302	55542	0.693106	51.8362	0.765600	−1
u_4	388	303	1.52744	77677	0.659480	42.6706	0.703328	−1

u_5	380	294	1.52778	70471	0.627972	42.3056	0.662990	0
u_6	209	230	1.069	35064	0.727834	57.6937	0.794246	−1
u_7	228	241	1.18788	39214	0.711268	55.7989	0.781472	−1
u_8	284	276	1.2821	54364	0.690350	51.8864	0.752902	−1
u_9	349	286	1.38822	63152	0.629686	44.5413	0.653802	0
u_{10}	356	286	1.49628	61489	0.601464	43.8237	0.639982	1
u_{11}	198	195	1.21924	25912	0.669246	52.5764	0.72167	0
u_{12}	229	222	1.32878	33977	0.666550	51.8413	0.708012	0
u_{13}	285	256	1.38284	47002	0.643292	48.4127	0.660664	0
u_{14}	356	272	1.55404	58891	0.606840	41.8819	0.620408	1
u_{15}	393	264	1.7982	62363	0.599000	37.0739	0.606300	1
u_{16}	225	192	1.318	29641	0.683952	46.1600	0.700376	0
u_{17}	264	207	1.52244	36261	0.660962	42.8283	0.685534	0
u_{18}	306	223	1.62578	43665	0.638984	40.0741	0.656882	1
u_{19}	397	240	2.06984	57250	0.599762	33.6936	0.610434	1
u_{20}	448	244	2.19004	64010	0.585122	30.5613	0.586980	1
u_{21}	222	184	1.45976	26597	0.647332	45.0595	0.677862	0
u_{22}	250	210	1.52088	33429	0.633874	45.7377	0.662322	0
u_{23}	323	222	1.77036	35481	0.617926	37.9395	0.621488	1

4.2 Knowledge mining based on VPTRS

In the rough fuzzy control method used to control the weld penetration, the goal of using rough-set knowledge mining was to find the minimum subset of frontal molten-pool features that could reflect the penetration state, and then to establish relationships between these important features and the penetration state. The equivalence relation between objects that is defined in classical Pawlak rough-set models is too strict and does not allow for any misclassification; thus, it is not very suitable for the modeling and analysis of welding processes. To improve the applicability of the rough-set theory to actual welding processes, a VPTRS was used to perform feature reduction and classification-rule extraction for the decision information system in Table 3. Therefore, corresponding relationships between the frontal molten-pool features and the penetration state could be established.

Unlike Pawlak rough sets, VPTRS feature reduction, which is based on tolerance relations, requires a calculation of the tolerance class of each sample, $u_i(i=1,2\cdots,23)$, in the feature space, U. While taking conditional feature c_7 as an example, the similarity threshold was set to $\tau=0.8$. According to Eqs. (1)–(4), the tolerance class, $S_{c_7}^{0.8}(u_i)$, of each sample, $u_i \in U$, can be expressed by Eq. (28):

$$\begin{cases} S_{c_7}^{0.8}(u_1)=\{u_1,u_2,u_6,u_7\} \\ S_{c_7}^{0.8}(u_2)=\{u_1,u_2,u_3,u_6,u_7,u_8\} \\ \cdots \\ S_{c_7}^{0.8}(u_{23})=\{u_5,u_9,u_{10},u_{13},u_{14},u_{15},u_{18},u_{19},u_{20},u_{22},u_{23}\} \end{cases} \quad (28)$$

The threshold of the misclassification rate was set to $\beta = 0.8$. By using Algorithm 1 to perform feature reduction for Table 3, a variable-precision tolerance β-reduction, $Red = \{c_7\}$,relative to d in the conditional feature set, $\{c_1, c_2, \cdots, c_7\}$,was obtained, as shown in Figure 4.

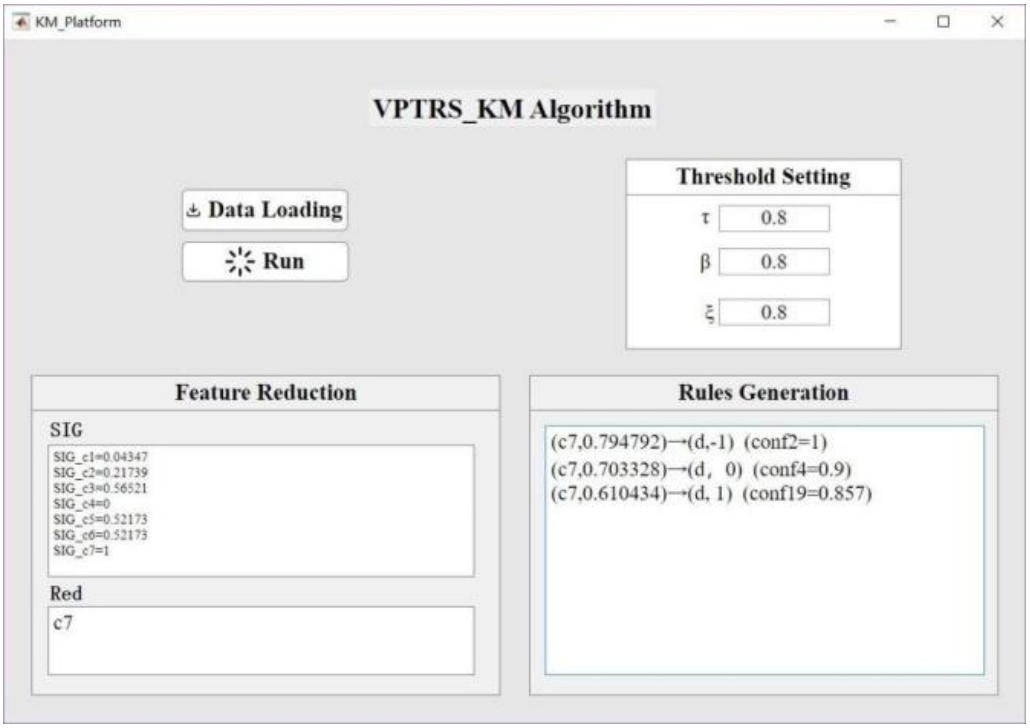


Fig.4. Molten-pool feature reduction and rule extraction based on VPTRS.

Figure 4 shows that, regarding the importance of each feature, $c_k\,(k = 1, 2, \cdots, 7)$, of the frontal molten pool with respect to the fusion state, d, the tail width ratio, c_7, had the highest importance. Furthermore, when only c_7 was retained, the classification capability was the same as that of the original decision information system. Therefore, this feature represents a minimum reduction in the feature space. In other words, the tail-width ratio is a frontal molten-pool feature that can characterize the fusion state.

To establish relationships between the features of the frontal molten pool and the fusion state, a rule-extraction algorithm, which was based on tolerance relations, was adopted on the basis of feature reduction to obtain the fusion classification rules. When the rule-generation threshold was set to $\xi = 0.8$, Algorithm 2 was used to obtain the following three rules:

$$r_2:\ (c_7, 0.794792) \to (d, -1) \qquad (Conf_2 = 1),$$
$$r_4:\ (c_7, 0.703328) \to (d, 0) \qquad (Conf_4 = 0.9),$$
$$r_{19}:\ (c_7, 0.610434) \to (d, 1) \qquad (Conf_{19} = 0.857).$$

These classification rules indicate that, during the welding process, as the width ratio of the molten-pool tail decreased, the weld depth gradually increased. In addition, the penetration state changed from incomplete penetration to complete penetration and then to excessive penetration; thus, the weld depth decreased monotonically with the tail-width ratio.

4.3 Establishment of the penetration control model

A fuzzy control model for weld penetration was established by taking a frontal molten-pool feature as the controlled variable. This feature was the tail-width ratio, which characterizes the weld penetration state. The inputs to the controller were the error, e, and the error change rate, ec, between the observed frontal molten-pool tail-width ratio, c_7, and the reference value, c_7^*. The output was the adjustment increment, Δi, of the welding current, as shown in Figure 5.

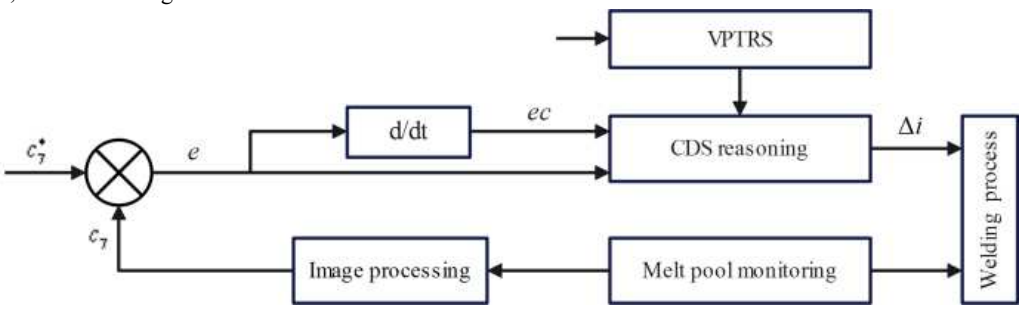


Fig.5. Weld-penetration control model based on rough fuzzy modeling and CDS reasoning.

The language values of the input and output variables were set to three levels: NB, ZE, and PB. Based on the correspondence relationships between the molten-pool depth and the tail-width ratio, as well as between the molten-pool depth and the welding current, it was inferred that the tail-width ratio of the molten pool decreased monotonically with the welding current. Therefore, a fuzzy control rule was established in which the tail-width ratio of the frontal molten pool was the controlled variable, as shown in Table 4.

Table 4 Fuzzy control rules

Δi/A		e		
		NB	ZE	PB
ec	NB	NB	NB	ZE
	ZE	NB	ZE	PB
	PB	ZE	PB	PB

Because of the limited practical experience of welders, it is difficult to establish a dense and complete control-rule base. In this study, symmetric similar triangular membership functions were used to define each linguistic value (fuzzy subset) of the input and output variables in the control rule. The universe of e was $[-0.08, 0.16]$, and the membership functions of each fuzzy subset for ec were the same as those for e, as shown in Figure 6. The membership functions of each linguistic value are provided in Eqs. (29)–(31):

$$NB(e)=\begin{cases}\dfrac{e+0.08}{0.02}, & e\in[-0.08,-0.06)\\ -\dfrac{e+0.04}{0.02}, & e\in[-0.06,-0.04]\end{cases} \tag{29}$$

$$ZE(e)=\begin{cases}\dfrac{e}{0.02}, & e\in[0,0.02)\\ \dfrac{0.04-e}{0.02}, & e\in[0.02,0.04]\end{cases} \tag{30}$$

$$PB(e)=\begin{cases}\dfrac{e-0.12}{0.02}, & e\in[0.12,0.14)\\ \dfrac{0.016-e}{0.02}, & e\in[0.14,0.16]\end{cases} \tag{31}$$

The universe of Δi was set to $[-40, 40]$ A, as shown in Figure 7, and the membership functions of each linguistic value are provided in Eqs. (32)–(34):

$$NB(\Delta i) = \begin{cases} \dfrac{\Delta i + 40}{7.5}, & \Delta i \in [-40, -32.5) \\ -\dfrac{\Delta i + 25}{7.5}, & \Delta i \in [-32.5, -25] \end{cases} \tag{32}$$

$$ZE(\Delta i) = \begin{cases} \dfrac{\Delta i}{7.5}, & \Delta i \in [0, 7.5) \\ \dfrac{15 - \Delta i}{7.5}, & \Delta i \in [7.5, 15] \end{cases} \tag{33}$$

$$PB(\Delta i) = \begin{cases} \dfrac{\Delta i - 25}{7.5}, & \Delta i \in [25, 32.5) \\ \dfrac{40 - \Delta i}{7.5}, & \Delta i \in [32.5, 40] \end{cases} \tag{34}$$

Figure 6 shows that the input regions for *e* and *ec* were not covered by the rule set. Therefore, if conventional inference methods, such as Mamdani inference, TSK inference, and similarity-based inference, are used, inappropriate or inaccurate results may be generated. In this study, fuzzy interpolation reasoning was used to solve the reasoning problem for scenarios with sparse rules.

By combining rough fuzzy modeling with CDS interpolation inference, an RF-CDS-based weld-penetration control system was constructed. The CDS algorithm included seven primary steps: input fuzzification, extraction of the input characteristic points, calculation of the characteristic distance ratio, construction of new rules, calculation of the characteristic similarity ratio, solving for the output characteristic values, and output defuzzification. In this system, the input variables, *e* and *ec*, were fuzzified using symmetric similar triangular membership functions and the output variables were fuzzified according to the maximum membership principle so that Δi could be determined.

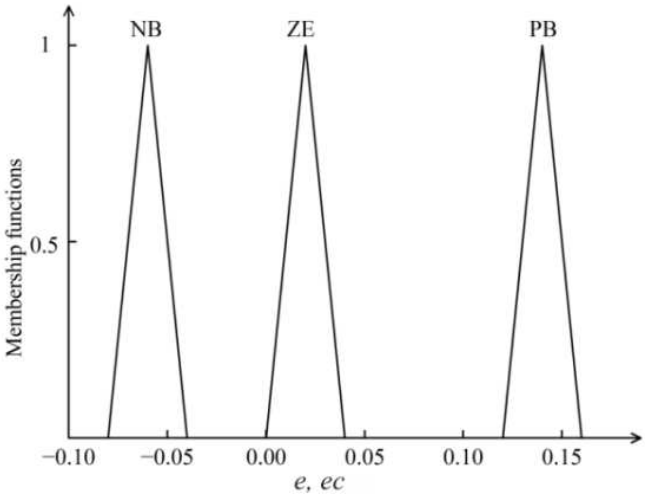


Fig.6. Membership functions of error and error change rate.

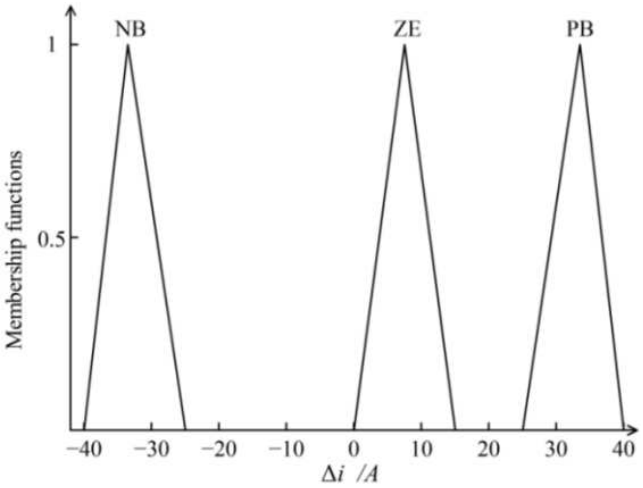


Fig.7. Membership functions of current adjustment increment.

4.4. Model testing and validation

The quality of weld-penetration forming is related to several process conditions, such as the groove angle, the root gap, and the root face. Of these, the root gap most significantly affects the penetration forming. In this study, the gap changes during the welding process were simulated through welding experiments to evaluate the rough fuzzy control model and the CDS interpolation inference algorithm when they were applied to weld-penetration forming.

The root gap of the workpiece in the experiments varied from 0.7 to 2.0 mm, as shown in Figure 8. The other process parameters are listed in Table 3. Experiments were conducted using RF-CDS controlled method. A CCD-camera sampling interval of 40 ms was utilized in the closed-loop control experiments. After the welding process was complete, the width of the molten pool on the back of the workpiece was measured to evaluate the weld-penetration effect.

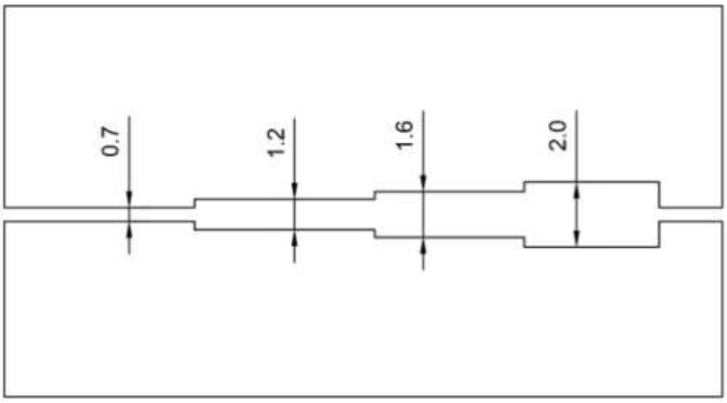


Fig.8. Distribution on root gap of workpiece.

According to the welding process library obtained from the experiments, the initial welding current was set to 185 A. During the welding process, the welding current and the tail-width ratio of the molten pool were measured under RF-CDS control conditions, as shown in Figure 9. During RF-CDS control, due to the response of the control system and the welding lag, the measured value of the molten-pool tail-width ratio was greater than the expected value during the initial stages of welding. When the welding current was adjusted through the controller,

the deviation between the measured and expected values of the tail-width ratio was small. Except for slight decreases when the gap changed, the tail-width ratio fluctuated around the expected value under closed-loop control conditions.

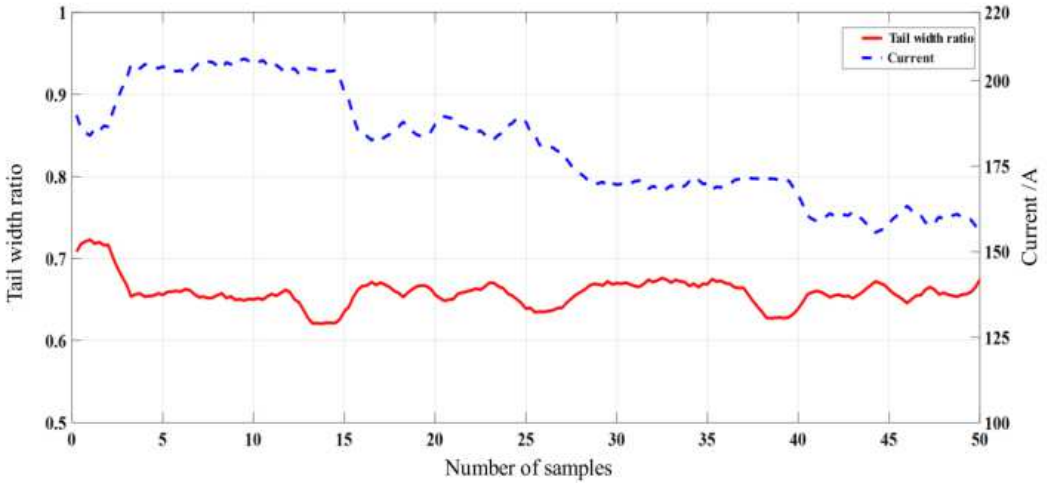


Fig.9. Changes in tail-width ratio of molten pool and current under RF-CDS control conditions.

The shapes of the back welds revealed that, under RF-CDS control conditions, due to the system response and welding hysteresis, there was a small amount of incomplete penetration on the back of the workpiece during the initial stages of welding. Subsequently, the width of the back of the weld remained essentially uniform and met the welding specification requirements of complete penetration, as shown in Figure 10.

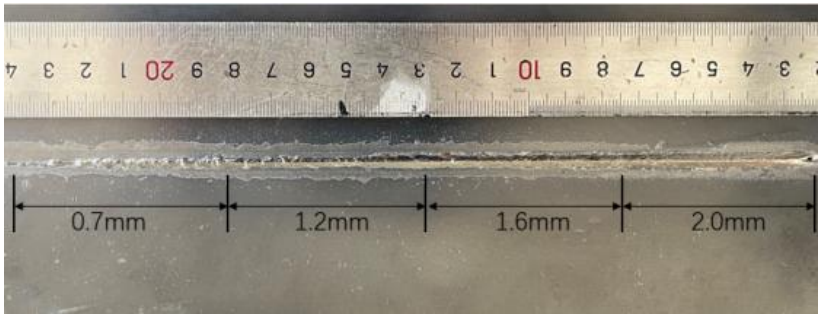


Fig.10. Penetration state of weld back under RF-CDS control conditions (welding direction: left to right).

4.5. Results and discussion

For the single-sided welding double-sided forming technology, penetration control has long been a difficult issue of concern in the welding industry. Researchers have attempted to seek breakthroughs via various models and algorithms, among which ANN-fuzzy-based control is a representative method in current welding penetration experimental research. It uses artificial neural networks to establish the relationship between the parameters of the frontal melt pool and the width of the back melt pool. During the welding process, the neural network can predict the penetration state based on the detected frontal information of the melt pool, and then feed the predicted results forward to a fuzzy controller to achieve penetration control by adjusting the welding parameters.

To test the effectiveness of the ANN-fuzzy-based control method, a control model for the back width of the molten pool is established using the dataset in Table 3. The neural network adopts a back propagation (BP) network with 8 hidden nodes, a learning rate of 0.01, and 400 epochs. The training curve and prediction accuracy

of the network are shown in Figure 11 and Figure 12, respectively. Figure 13 indicates the forming state of the back of the workpiece after welding.

From Figure 13, it can be seen that the welded workpiece under ANN-fuzzy-based control is almost in an incomplete penetration state at a gap of 0.7 mm (i.e., the back width of the weld is zero), after which the width of the back weld gradually increases from zero and tends to be uniform. The main reason for the occurrence of a large amount of incomplete penetration at small gaps is the significant deviation between the ANN predicted values and the actual values of the weld back width (as shown in Figure 12), which leads to insufficient increase in welding current during the control process.

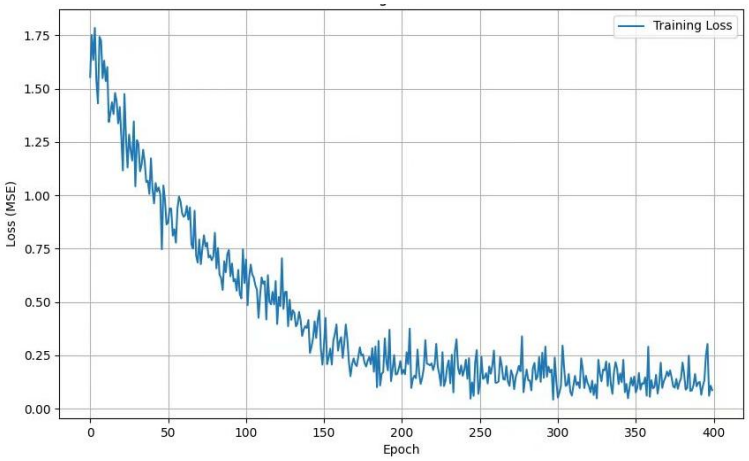


Fig. 11. Training loss curve of ANN

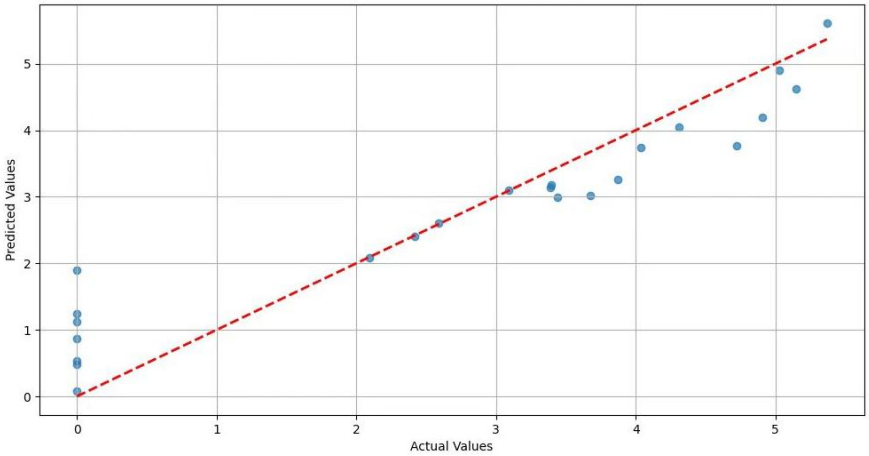


Fig. 12. Predicted values of ANN versus actual values

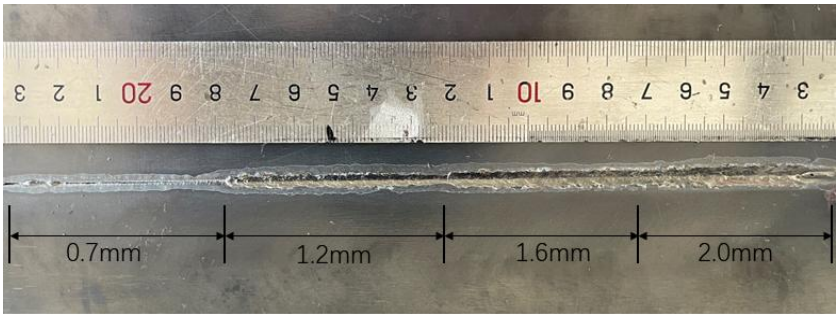


Fig. 13. Penetration state of weld back under ANN-fuzzy-based control conditions (welding direction: left to right).

As mentioned earlier, in practical operations, experienced welders often determine the penetration state based on certain geometric features of the observed frontal melt pool, and then control the penetration depth by adjusting the welding electrical parameters. From the welders' manipulation actions, it can be seen that a key step in achieving intelligent control of melt penetration is to find geometric features that can characterize the melt penetration state from the observed frontal information of the melt pool.

In this section, we used a case study to illustrate how to find melt pool features that can characterize the melting state. To ensure the representativeness of the data in the case analysis, two process parameters (i.e. weld gap and welding current) that significantly affect penetration in one-sided welding double-sided forming were selected, and seven feature parameters commonly-used to describe the shape and size of the melt pool were extracted.

Through data collection, feature extraction, feature reduction, and rule generation, an important feature that can characterize the melting state - the tail width ratio of the molten pool - was obtained. This feature parameter is mainly used to describe the shape of the latter half of the molten pool. When the weld is in a molten state, the tail of the frontal melt pool becomes thinner and longer, indicating that the weld bead on the back of the melt pool has been formed. The results of the case study indicate that, in terms of methodology, data analysis based on rough set theory may effectively uncover certain implicit relationships or patterns in the dataset. This will help discover key features that characterize the melting state from the frontal information of the melt pool, and provide a new feasible approach for achieving melting control.

5. Conclusions

This study produced four primary conclusions:

(1) Penetration control is an important component of the forming quality control during welding. A feasible method of achieving intelligent control of the fusion process is to simulate the behavior of a human welder by seeking and establishing correspondence relationships between the key features of the frontal molten pool and the penetration state. This paper proposed a weld-penetration control method that combined knowledge mining of variable-precision tolerance rough sets, fuzzy logic modeling, and fuzzy interpolation reasoning techniques.

(2) Classical rough sets cannot directly process continuous data and cannot handle noisy data well. By constructing a variable-precision tolerance rough-set model, a fast-reduction algorithm that was based on feature importance was established and a classification-rule extraction algorithm was derived from tolerance relations. This model can effectively handle continuous data that contains noise and thereby enhances the adaptability of rough sets to practical systems.

(3) To address the inference problem that occurs under incomplete or sparse fuzzy rule-base conditions, an interpolation inference algorithm was developed based on characteristic distance and similarity (CDS). It begins by extracting geometric characteristics of fuzzy sets, then it solves the characteristics of conclusions using several

steps, such as the construction of feature distance ratios, the establishment of new rules, and the calculation of feature similarity ratios. The proposed algorithm is simple and computationally efficient. It also satisfies the normal convexity and reducibility of inference results.

(4) Welding experiments were also conducted. The process conditions and welding specifications were systematically changed during these experiments so that a penetration-state decision information system could be established. By utilizing the variable-precision tolerance rough-set feature-reduction and rule-extraction algorithms, correspondence relationships between the characterization features of the frontal molten pool and the penetration state were obtained; thus, a weld penetration control system could be constructed through fuzzy logic modeling and interpolation reasoning techniques. Welding experiments with root-gap step changes were conducted to verify the effectiveness of the system. The experimental results showed that, under closed-loop control conditions, the molten pool formed well and met the basic requirements of welding-process specifications.

References

[1]Wang K H, Gao F, and Gao J P. The status and development of intelligent welding robot based on visual technology [J]. Machine Building & Automation, 2010, 39(5): 1-6.

[2]Wang G Y, Yao Y Y, and Yu H. A survey on rough set and applications [J]. Chinese Journal of Computers, 2009, 32(7): 1229-1246.

[3]Chen Q, Pan J L, and Osima K. Fuzzy control in welding process [J]. Chinese Journal of Mechanical Engineering, 1995, 31(4): 86-91.

[4]Li F Y, Li Y, and Yang J. Fuzzy rule-based interpolative reasoning: a survey [J]. Chinese Journal of Computers, 2022, 45(8): 1688-1711.

[5]Xiong J, and Zou S. Active vision sensing and feedback control of back penetration for thin sheet aluminum alloy in pulsed MIG suspension welding [J]. Journal of Process Control, 2019, 77: 89-96.

[6]Yan X. Study on Visual Inspection and Control Technology of fusion hole TIG single side welding with back formation [D]. Jinan: Shandong University, 2021.

[7]Li L Y, Chen H Y, and Dong Y, et al. Penetration recognition and close-loop control method of fast-frequency pulsed TIG welding process for 304 stainless steel [J]. Electric Welding Machine, 2023, 53(9):47-54+60.

[8]Pan Q. Visual sensing of fusion hole and penetration closed-loop control in thin plate high frequency pulsed TIG welding [D]. Jinan: Shandong University, 2023.

[9]Liu Y K, Zhang W J, and Zhang Y M. Dynamic neu-ro-fuzzy-based human intelligence modeling and control in GTAW [J]. IEEE Transactions on Automation Science and Engineering, 2013, 12(1): 324-335.

[10]Wang Z, Zeng Z, and Wu S, et al. Weld penetration control of wire-filled pulsed gas tungsten arc welding of pipe in the horizontal position [J]. Welding in the World, 2023: 1-15.

[11]Bai P F. Detection and analysis of penetration information in pulsed gas metal arc welding [D]. Tianjin: Tianjin University, 2018.

[12]Chen Z, Chen J, and Feng Z. Welding penetration prediction with passive vision system [J]. Journal of Manufacturing Processes, 2018, 36: 224-230.

[13]Li W, Wu J, and Hu T, et al. Rough set based modeling for welding groove bottom state in narrow gap MAG welding [J]. Industrial Robot: An International Journal, 2015, 42(2): 110-116.

[14]Chen G. Research on the process parameter decision method of hull sub-assembly welding based on knowledge modeling [D]. Shanghai: Shanghai Jiao Tong University, 2021.

[15]Li W H, Li Q, and Yang F, et al. An intelligent modeling method for welding deviation of rotating arc NGW [J]. Applied Mechanics and Materials, 2013, 312: 805-809.

[16]Zhong J Y. Study on robot Aluminum Alloy Pulse GTAW seam tracking and forming quality control [D]. Shanghai: Shanghai Jiao Tong University, 2017.

[17]Chao Y S, and Sun W L. Welding type oriented association rules acquisition based on rough sets [J]. Computer Engineering & Applications, 2015, 51(15): 244-248+260.

[18]Wang C S, Zou L, and Yang X H. Analysis of fatigue life factors of aluminum alloy welded joints based on neighborhood rough set theory [J]. Journal of Jilin University (Engineering and Technology Edition), 2017, 47(6): 1848-1853.

[19]Jiang W. Attribute reduction of neighborhood rough set based on improved fish swarm algorithm and its application [D]. Dalian: Dalian Jiao Tong University, 2020.

[20]Wu Y Q, Yuan Z H, Wang J H. A fuzzy controller design of seam tracking for welding robot [J]. Advanced Materials Research, 2012, 442: 370-374.

[21]Wang Z, Wang X, and Gao W X, et al. Research on fuzzy incremental control for submerged arc weld with image processing [J]. Measurement & Control Technology, 2016, 35(12): 62-65+70.

[22]Wang P, Zhang D, Lu B. Robust fuzzy sliding mode control based on low pass filter for the welding robot with dynamic uncertainty [J]. Industrial Robot: the international journal of robotics research and application, 2020, 47(1): 111-120.

[23]Kóczy L T, and Hirota K. Interpolative reasoning with insufficient evidence in sparse fuzzy rule bases [J]. Information Sciences, 1993, 71(1): 169-201.

[24]Guo B, Li S, and Tang Q, et al. A fuzzy interpolation cross-correlation method for time-delay estimation of partial discharge UHF pulse signals [J]. Journal of Electrical and Computer Engineering, 2021, 2021: 1-10.

[25]Molnárka G I, Kovács S, and Kóczy L T. Fuzzy rule interpolation based fuzzy signature structure in building condition evaluation [C]. 2014 IEEE International Conference on Fuzzy Systems (FUZZ-IEEE). IEEE, 2014: 2214-2221.

[26]Ofor W D, Nwiabu N D, and Matthias D. Face detection and expression recognition using fuzzy rule interpolation [J]. International Journal of Computer Sciences and Engineering, 2019, 7(5): 1683-1689.

[27]Szili F Á, Botzheim J, and Nagy B. Bacterial evolutionary algorithm-trained interpolative fuzzy system for mobile robot navigation [J]. Electronics, 2022, 11(11): 1734.

[28]Yang J, Shang C, and Li Y, et al. Anfis construction with sparse data via group rule interpolation [J]. IEEE Transactions on Cybernetics, 2019, 51(5): 2773-2786.

[29]Li F, Shang C, and Li Y, et al. Interpretable mammographic mass classification with fuzzy interpolative reasoning [J]. Knowledge-Based Systems, 2020, 191: 105279.

[30]Fan C J. Weld pool characters extraction and intelligent control during varied gap aluminum alloy pulsed GTAW process [D]. Shanghai: Shanghai Jiao Tong University, 2008.

[31]Skowron A. Tolerance approximation spaces [J]. Fundamenta Informaticae, 1996, 27(2/3): 245-253.

[32]Ziarko W. Variable precision rough set model [J]. Journal of Computer and System Sciences, 1993, 46(1): 39-59.

Funding

Supported by National Natural Science Foundation of China (Grant No. 52261044), and Guangxi Key Research and Development Program Project of China (Grant No. AB25069344,FN2600640627)，and Research Foundation Ability Enhancement Project for Young and Middle aged Teachers in Guangxi Universities of China (Grant No. 2025KY0479),and Qinzhou scientific research and technology development plan project of China (Grant No. 20241422).

Author contributions

Conceptualization, X.L.; data curation, N.F. and X.L；funding acquisition, X.L.and Z.F.; validation ,N.F. and S.W.; methodology, X.L. and Z.F.; software, X.L. and S.W.; supervision, X.L. and S.W.; visualization, X.L. and Z.F.; writing—original draft, X.L. and Z.F.; writing—review and editing, X.L., Z.F. and N.F.. All authors have read and agreed to the published version of the manuscript.

Data Availability Statement

All data generated or analyzed during this study are included in this article.

Acknowledgements

Not applicable.